EPJ Web of Conferences **175**, 12010 (2018) https://doi.org/10.1051/epjconf/201817512010
Lattice 2017

Lattice study of area law for double-winding Wilson loops

Akihiro Shibata[1,⋆], *Seikou* Kato[2], *Kei-Ichi* Kondo[3], and *Ryutaro* Matsudo[4]

[1] *Computing Research Center, High Energy Acceleration Research Organization (KEK), Oho 1-1, Tsukuba 305-0801, Japan*
[2] *Oyama National College of Technology, Oyama 323-0806, Japan*
[3] *Department of Physics, Faculty of Science, Chiba University, Chiba 263-8522, Japan*
[4] *Department of Physics, Faculty of Science and Engineering, Chiba University, Chiba 263-8522, Japan*

Abstract. We study the double-winding Wilson loops in the SU(N) Yang-Mills theory on the lattice. We discuss how the area law falloff of the double-winding Wilson loop average is modified by changing the enclosing contours C1 and C2 for various values of the number of color N. By using the strong coupling expansion, we evaluate the double-winding Wilson loop average in the lattice SU(N) Yang-Mills theory. Moreover, we compute the double-winding Wilson loop average by lattice Monte Carlo simulations for SU(2) and SU(3). We further discuss the results from the viewpoint of the Non-Abelian Stokes theorem in the higher representations.

1 Introduction

The Wilson loop is a gauge-invariant and important operator for the lattice study. By using a single winding Wilson loop, we investigate the static potential and the flux tube between quark and antiquark in the fundamental representation. We further investigate the evidence of the dual superconductivity such as the restricted field dominance and the magnetic monopole dominance for the string tension and dual Meissner effect.

There still exist two promising mechanisms for quark confinement. One is the dual superconductivity [1] in which the magnetic monopole plays a dominant role for confinement. The other is the vortex picture in which the center vortex plays a relevant role for confinement [2]. Recently, Greensite and Hölwieser presented the testing method for the mechanism of confinement by using the double-winding Wilson loop which enclosing contours are in the same plain [3]. For the $SU(2)$ case, they investigate the average of the double-winding Wilson loop made of Yang-Mills field, the center field extracted in the maximal center gauge, and the Abelian-projection field in the maximal Abelian gauge. They showed that the string tension for the minimum surface of the Wilson loop is the difference of area behavior in case of the center-projection field as well as the Yang-Mills field and the center-projection. In case of Abelian-projected field, the string tension is the sum of area behavior in the same way as the Abelian case. However, it must be examined whether replacing the Yang-Mills field with the Abelian-projected field in the Wilson loop operator leads to the correct result or not in view of the non-Abelian Stokes theorem.

⋆ Speaker, e-mail: akihiro.shibata@kek.jp

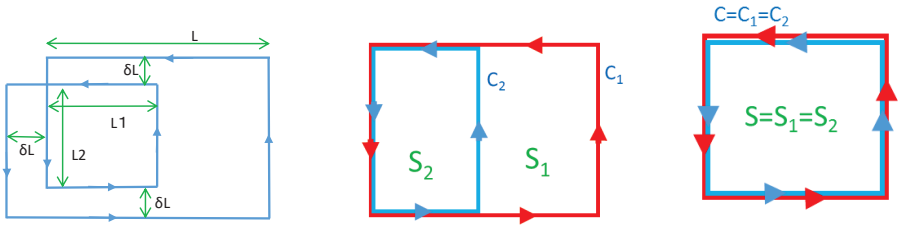

Figure 1. The contour of the double-winding Wilson loop. The contour $C = C_1 \times C_2$ winds once around a loop C_1 and once around a loop C_2 in the same direction. The loop C_1 lies entirely in the minimal area of the loop C_2. S_1 and S_2 represent the minimum areas formed by C_1 and C_2, respectively. (leftmost) The parametrization of the contours of the double-winding Wilson loop. (center) The $\delta L = 0$ case. (rightmost) The the double-winding Wilson loop with the identical countour, i.e., the two identical loop, $C_1 = C_2$.

In this talk, we investigate the double-winding Wilson loops of SU(N) Yang-Mills theory on the lattice to know the correct behavior of the expectation values such as the gauge group dependence, the relation to N-ality, and the relation to the non-Abelian stokes theorem in view of the dual superconductivity.

2 Double-winding Wilson loop

We set up the double-winding Wilson loop on the lattice $W(C)$ (see Figure 1). The contour $C = C_1 \times C_2$ winds once around a loop C_1 and once around a loop C_2 in the same direction, where the two coplanar loops C_1 and C_2 share one point in common. The loop C_2 lies entirely in the minimal area of the loop C_1. The area S_1 represents the minimum area formed by C_1, i.e., $S_1 = L \times L_2 + \delta L \times (2L + L_2 + \delta L)$. The area S_2 represents the minimum areas formed by C_2, i.e., $S_2 = L_1 \times L_2$. For simplicity of the analysis, we sometimes use the case of $\delta L = 0$ (the center panel). The rightmost panel represents the double-winding Wilson loop with an identical contour (two identical loops, $C_1 = C_2$, or $\delta L = 0$ and $L_1 = L$).

We investigate how the area law falloff of the double-winding Wilson loop average is modified by changing the enclosing contours C_1 and C_2 for various values of the number of color N_c in $SU(N_c)$-Yang-Mills theory. We first study the double-winding Wilson loop average by using the strong-coupling expansion. Then, we evaluate the double-winding Wilson loop average for $SU(2)$ and $SU(3)$ by using Monte-Carlo simulations to examine the results of the strong-coupling expansion and the calculation in the continuum theory [4].

3 Strong Coupling expansion

By using the strong coupling expansion [5], we evaluate the double-winding Wilson loop average in the lattice $SU(N_c)$ Yang-Mills theory. For simplicity of calculation, we consider the $\delta L = 0$ case of Fig. 1. We adopt the Wilson standard action

$$S_g = \beta \sum_{x,\mu} \mathrm{Re}\,\mathrm{tr}\left(1 - U_p\right), \quad U_p = U_{x,\mu} U_{x+\mu,\nu} U^{\dagger}_{x+\nu,\mu} U^{\dagger}_{x,\nu} \tag{1}$$

where $U_{x,\mu}$ ($\in SU(N_c)$) is a gauge link variable, and $\beta = 2N_c/g^2$ is the gauge coupling parameter. We consider the case $\beta \ll 1$ ($g \gg 1$) and the average of the double-winding Wilson loop average is

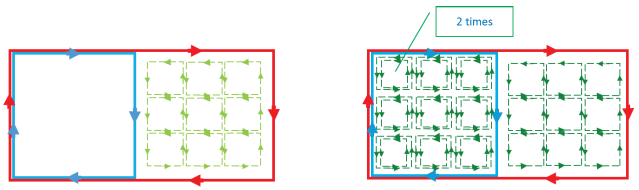

Figure 2. strong coupling expansion: contributing graph for $SU(2)$ case

calculated by expansion of β. For simplicity of calculation, we investigate the case of $\delta L = 0$, i.e., the center panel of Fig.1. The $SU(N_c)$ group integrals are given as follows [6][7]

$$\int dU = 1 \tag{2a}$$

$$\int dU U_{ab} = 0 \tag{2b}$$

$$\int dU U_{ab} U^{\dagger}_{cd} = \frac{1}{N_c}\delta_{ad}\delta_{bc} \tag{2c}$$

$$\int dU U_{a_1b_1} U_{a_2b_2} \cdots U_{a_Nb_{N_c}} = \frac{1}{N_c!}\epsilon_{a_1a_2\cdots a_{Nc}}\epsilon_{b_1b_2\cdots b_{N_c}} \tag{2d}$$

$$\int dU U_{a_1b_1} U_{a_2b_2} \cdots U_{a_Mb_M} = 0 \quad (M \neq 0 \bmod N_c\ ) \tag{2e}$$

$$\begin{aligned}\int dU U_{ab} U_{cd} U^{\dagger}_{ij} U^{\dagger}_{kl} &= \frac{1}{4}\delta_{2,Nc}\ \epsilon_{ac}\epsilon_{bd}\epsilon_{ik}\epsilon_{jl} \\ &+ \frac{1}{N_c^2-1}\left[\delta_{aj}\delta_{bi}\delta_{cl}\delta_{dk} + \delta_{al}\delta_{bk}\delta_{ci}\delta_{di} - \frac{1}{N_c}\left(\delta_{aj}\delta_{bk}\delta_{cl}\delta_{di} + \delta_{al}\delta_{bi}\delta_{cj}\delta_{dk}\right)\right]\end{aligned} \tag{2f}$$

Figure 2 shows the examples which contribute to the expectation of the double-winding Wilson loop. The leading term of the expansion is given by the planar diagram that covers the minimal areas S_1 and S_2.

SU(2) case : The leading contribution is given by the leftmost diagram of Fig.2. The area S_2 is not fulfilled by plaquettes, and we have only contribution from area $S_1 - S_2$. Thus we have the difference-of-area behavior:

$$W(C)|_{\text{Leading}} = -2\left(\frac{\beta}{N_c}\right)^{S_1-S_2}. \tag{3}$$

The right diagram of Fig.2 is the higher order term, which gives the sum-of-area behavior:

$$W(C)|_{\text{right}} = -q_{N_c}(S_2)\left(\frac{\beta}{N_c}\right)^{S_1+S_2}, \tag{4}$$

where the coefficient $q_{N_c}(S)$ is given by

$$q_{Nc}(S) = \frac{N_c^2}{2}\left[\left(\frac{N_c}{N_c-1}\right)^{S-1} - \left(\frac{N_c}{N_c+1}\right)^{S-1}\right]. \tag{5}$$

As for $U(1)$ case it should be noticed that the average of the left panel of Fig.2 vanishes in the $U(1)$ case, and the leading term starts from the right panel. Therefore, we have the sum-of-area behavior.

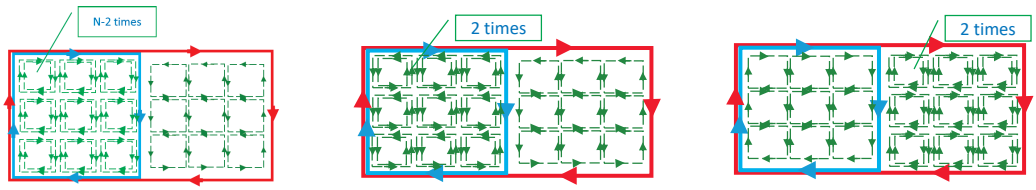

Figure 3. strong coupling expansion: contributing graph for $SU(N_c)$ $N_c \geq 3$. The rightmost panel is only for $SU(3)$ case

SU(3) case : The leading term is given by the left panel of Fig.3.

$$W(C)|_{\text{Leading}} = -2\left(\frac{\beta}{N_c}\right)^{S_1}. \tag{6}$$

The higher corrections are given by the center and rightmost diagrams of Fig.3

$$W(C)|_{\text{correction}} = -q_{N_c}(S_2)\left(\frac{\beta}{N_c}\right)^{S_1+S_2} - q_{N_c}(S_1 - S_2)\left(\frac{\beta}{N_c}\right)^{2S_1-S_2}. \tag{7}$$

The area law is neither the neither difference-of-area behavior nor the sum-of-area behavior.

SU(4) case : For $N_c = 4$, the left and center diagrams in Fig.3 give the same contribution:

$$W(C)|_{\text{Leading}} = -2q_{N_c}(S_2)\left(\frac{\beta}{N_c}\right)^{S_1+S_2}. \tag{8}$$

SU($\mathbf{N_c}$) $\dot{N_c} \geq 5$ **case :** For $N_c \geq 5$, the leading diagram is interchanged, and the center diagram in Fig.3 is the leading term:

$$W(C)|_{\text{Leading}} = -q_{N_c}(S_2)\left(\frac{\beta}{N_c}\right)^{S_1+S_2}. \tag{9}$$

4 Numerical simulation

We perform the numerical simulation on the lattice by using the Wilson action. For $SU(2)$ case, we generate 1000 configurations for 32^4 lattice with $\beta = 2.6$ by using the standard pseudo heat-bath method. For $SU(3)$ case, we generate 1000 configurations for 24^4 lattice with $\beta = 6.2$ by using Cabibo-Marinari[8] and over-relaxation algorithms. In the measurement of the Wilson loop average, the gauge links are smeared by using the APE smearing method [9].

4.1 SU(2) case

First, we investigate the double-winding Wilson loop for the $SU(2)$ case. The double-winding Wilson-loop operator, $W(C = C_1 \times C_2)$, is represented at the center panel of Fig. 1. Note that the case of $L_1 = 0$ corresponds to the single-winding Wilson loop ($C = C_1$), and the $L_1 = L$ case corresponds to the case of the two identical loops. We measure the expectation value of the Wilson loop $\langle W(C) \rangle$ for various

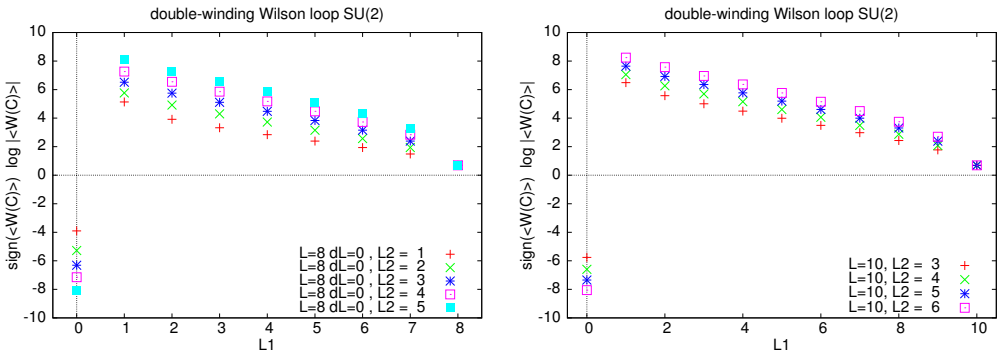

Figure 4. The measurement of the Wilson loop average of Fig. 1 ($\delta L = 0$) for the $SU(2)$ case : The left and right plots represent sign($\langle W(C)\rangle$)log($|\langle W(C)\rangle|$) v.s. L_1 for $L = 8$ and $L = 10$, respectively. The case of $L_1 = 0$ corresponds to the single-winding Wilson loop ($C = C_1$), and the case of $L_1 = L$ corresponds to the double-winding Wilson loop with identical contours (the rightmost panel of Fig. 1 , $C_1 = C_2$).

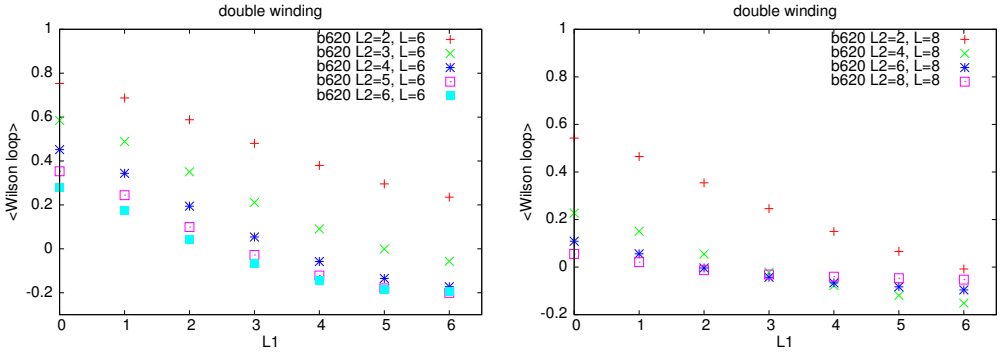

Figure 5. The measurement of the double-winding Wilson loop for the SU(3) case. ($\delta L = 0$) The left and right panels show the plots $\langle W(C)\rangle$ v.s. L_1 for $L = 6$ and $L = 8$, respectively. The case of $L_1 = 0$ and $L_1 = L$ represents the single-winding Wilson loop, and the double-winding Wilson loop with identical contours, respectively.

L_1, L_2 with fixed L. As L_1 increases with fixed L and L_2, S_1 is constant, S_2 increases, and then $S_1 - S_2$ decreases. The result is shown in Figure 4. The vertical axis represents the logarithmic-scale Wilson loop average as sign($\langle W(C)\rangle$) log($|\langle W(C)\rangle|$). The left and right panels show the case of $L = 8$ and $L = 10$, respectively. The Wilson loop average changes sign for the case of the single-winding loop and the double-winding loop, i.e., in the case of $L_1 = 0$, the Wilson loop average $\langle W(C)\rangle$ takes positive value with $|\langle W(C)\rangle| \leq 1$, while, in the case of $L_1 \neq 0$, the Wilson loop average takes a negative value with $|\langle W(C)\rangle| \leq 1$. The plots show that the absolute value of the double-winding Wilson loop average falls off as L_1 increases. This result is consistent with the result in the strong coupling expansion: The Wilson loop average falls off as the difference-of-area behavior.

4.2 SU(3) case

We investigate the $SU(3)$ case. Figure 5 shows the Wilson loop average for $\delta L = 0$, for various L_1 and L_2. The left panel shows the case of $L = 6$. As L_1 increases, the Wilson loop average decreases.

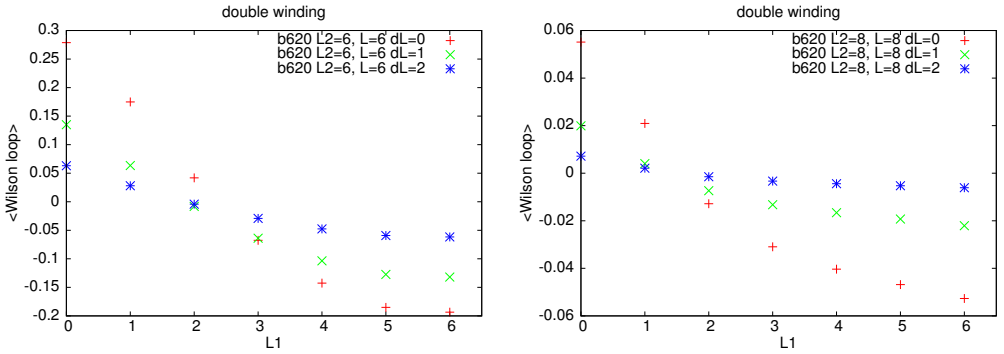

Figure 6. The measurement of the double-winding Wilson loop average for the SU(3) case. The left and right panel show δL dependence of $\langle W(C)\rangle$ v.s. L_1 for $L = L_2 = 6$ and $L = L_2 = 8$, respectively. The case of $L_1 = 0$ corresponds to the single-winding Wilson loop.

For a small area of S_1 $\langle W(C)\rangle$ is positive, while for large area of S_1 $\langle W(C)\rangle$ decreases to negative value as L_1 increases. The right panel shows the case of $L = 8$. As L_1 increases, the Wilson loop average decreases. However, for large area of S_1, $\langle W(C)\rangle$ decreases slowly from $\langle W(C_1)\rangle$ (> 0) to $\langle W(C_1 \times C_1)\rangle$ (< 0) as L_1 increases. In case of large S_1 and S_2, the Wilson loop average $\langle W(C)\rangle$ is negative and almost constant. The double-winding Wilson loop for the $SU(3)$ case obeys the area law of S_1.This result is consistent with the strong-coupling expansion.

Next we investigate the case of $\delta L \neq 0$ (see left panel of Fig. 1). Figure 6 shows measurement of the double-winding Wilson loop average for various δL. As is the same with the case of $\delta L = 0$, $\langle W(C)\rangle$ deceases from $\langle W(C_1)\rangle$ (> 0) as L_1 increases. For large S_1 and S_2, the Wilson loop average $\langle W(C)\rangle$ is negative and almost constant. Therefore, the double-winding Wilson loop average is independent of L_1 (S_2), and it follows the area law of the area enclosed by C_1, i.e., S_1.

5 Double-winding Wilson loop with an identical contour

We finally discuss the double-winding Wilson loop with an identical contour ($C_1 = C_2 = C$) (See the rightmost panel of Fig.1). This can be rewritten by using the Wilson loops in the irreducible representations [4] :

SU(2) case : $2 \otimes 2 = 2 \otimes 2^* = 1 \oplus 3$

$$\langle W(C \times C)\rangle = -\frac{1}{2} + \frac{3}{2}\left\langle W_{\rm adj}(C)\right\rangle \tag{10a}$$

SU(3) case : $3 \otimes 3 = 3^* \oplus 6$

$$\langle W(C \times C)\rangle = -\left\langle W_{[0,1]}(C)\right\rangle + 2\left\langle W_{[2,0]}(C)\right\rangle \tag{10b}$$

SU(N) case : $N \otimes N = \left(\frac{N(N-1)}{2}\right)_A \oplus \left(\frac{N(N+1)}{2}\right)_S$

$$\langle W(C \times C)\rangle = -\frac{N-1}{2}\left\langle W_{[0,1,\ldots,0]}(C)\right\rangle + \frac{N+1}{2}\left\langle W_{[2,0,\ldots,0]}(C)\right\rangle \tag{10c}$$

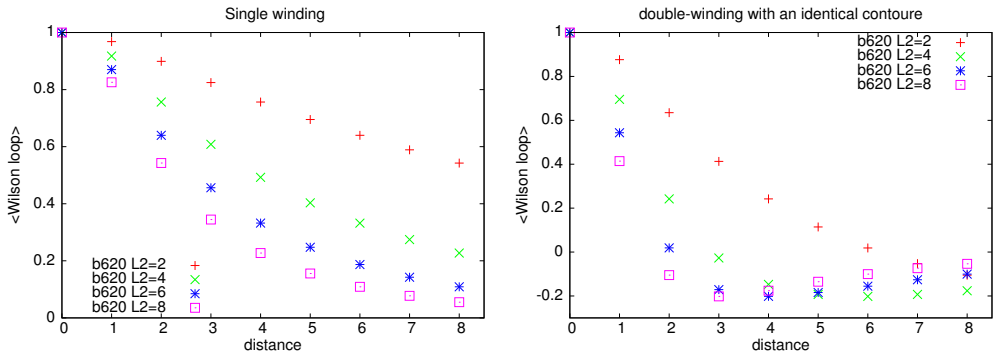

Figure 7. (left) The single-winding Wilson loop (right) the double-winding Wilson loop with identical contour.

Here the representation is specified by the Dynkin indices, e.g., the (anti)fundamental representation $\mathbf{3}^*$ with the Dynkin index $[0,1]$, the sextet representation $\mathbf{6}$ with the Dynkin index $[2,0]$. If one assumes the Casimir scaling of the string tension, one can estimate the double-winding Wilson loop average,

$$\langle W_R(C)\rangle \simeq \exp(-S\sigma_R) \quad \text{with } \sigma_R = \frac{C_2(R)}{C_2(F)}\sigma_F, \tag{11}$$

where σ_F, σ_R, $C_2(F)$, and $C_2(R)$ denote the string tension of the fundamental representation (F) and the representation R, and the quadratic Casimir operator of the fundamental representation and the representation R, respectively.

In the calculation of the strong-coupling expansion, the Wilson loop average can be estimated for large area S. Therefore, the Wilson-loop average in the lower dimensional representation become dominant for large area S, that is, the first term in each eq(10) becomes dominant. These results are consistent with results in strong coupling expansion.

Next, we examine the relation eq(10b) by the numerical simulations. Figure 7 shows the Wilson loop averages of the single-winding Wilson loop for the fundamental representation (left panel) and the double-winding Wilson loop with the identical contour (right panel) for the $SU(3)$ case. The single-winding Wilson-loop average of the representation R is positive and it falls off monotonically as the area S increases. However, the double-winding Wilson0loop average decreases as the area S increases, and changes the sign from positive to negative. As S further increases, the absolute value of the Wilson-loop average decreases to zero. These are consistent with eq(10b), because the second term $\langle W_{[2,0]}(C)\rangle$ in eq(10b), is dominant for small S, and fall off quickly as S increases. For larger S, the dominant term is switched from the second one to the first one.

6 Summary and discussion

We have investigated the double-winding Wilson loop average for $SU(N_c)$ Yang-Mills theory by using the strong coupling expansion and the lattice simulation. By using the strong coupling expansion, we obtain the difference-of-area behavior for the $SU(2)$ case. For the $SU(N_c)$ ($N_c \geq 3$) case, however, the area law is the neither difference-of-area behavior nor sum-of-area behavior. By using numerical simulation, we have confirmed the result of the strong coupling expansion for the Wilson loop with large areas S_1 and S_2. These results are consistent with the results from the continuum theory [4] .

We are further interested in the dual superconductivity in the higher dimensional representation of quarks. It has been pointed out that naively replacing the Yang-Mills field with the Abelian projected field cannot reproduces the correct result [3]. In order to confirm the dual superconductivity, we should go back to the non-Abelian Stokes theorem (NAST) for the higher-dimensional representation [10], and derive the Wilson-loop operator with the restricted ("Abelian") field that can reproduce the area law in the NAST. These studies will appear in near future works.

Acknowledgement

A.S and K.-I. K. were supported by Grant-in-Aid for Scientific Research, JSPS KAKENHI Grant Number (C) No.15K05042. R. M. was supported by Grant-in-Aid for JSPS Research Fellow Grant Number 17J04780. The numerical calculations are supported by the Large Scale Simulation Program No.16/17-20(2016-2017) of High Energy Accelerator Research Organization (KEK).

References

[1] Y. Nambu, Phys. Rev. D10, 4262(1974); G. 't Hooft, in High Energy Physics, edited by A. Zichichi (Editorice Compositori, Bologna, 1975); S. Mandelstam, Phys. Report 23, 245(1976); A.M. Polyakov,Nucl. Phys. B120, 429(1977).
[2] J. Greensite, Lect. Notes Phys. 821 (2011) 1-211
[3] J. Greensite, R. Höllwieser, Phys. Rev. D91 (2015) no.5, 054509
[4] R. Matsudo and K.-I. Kondo Phys. Rev. D96 (2017) no.10, 105011
[5] K.G. Wilson, Phys. Rev. D10 (1974) 2445
[6] M. Creutz, "Quarks, Gluons and lattice", Cambrridge University Press, 1983
[7] M.Creutz, Rev. Mod. Phys. 50 (1978), 561
[8] N. Cabibbo and E. Marinari, Phys. Lett. B119 (1992) 387-390
[9] APE collaboration, M. Albanese et al., Phys. Lett. B 192 (1987) 163.
[10] R.Matsudo and K.-I. Kondo, Phys. Rev. D92 (2015) no.12, 125038